



**HAL**  
open science

## Cellulose, proteins, starch and simple carbohydrates molecules control the hydrogen exchange capacity of bio-indicators and foodstuffs

A-L. Nivesse, N. Baglan, Gilles F Montavon, G. Granger, O. Péron

► **To cite this version:**

A-L. Nivesse, N. Baglan, Gilles F Montavon, G. Granger, O. Péron. Cellulose, proteins, starch and simple carbohydrates molecules control the hydrogen exchange capacity of bio-indicators and foodstuffs. *Chemosphere*, 2021, 269, pp.128676. 10.1016/j.chemosphere.2020.128676 . hal-03139246

**HAL Id: hal-03139246**

<https://hal.science/hal-03139246v1>

Submitted on 9 Mar 2023

**HAL** is a multi-disciplinary open access archive for the deposit and dissemination of scientific research documents, whether they are published or not. The documents may come from teaching and research institutions in France or abroad, or from public or private research centers.

L'archive ouverte pluridisciplinaire **HAL**, est destinée au dépôt et à la diffusion de documents scientifiques de niveau recherche, publiés ou non, émanant des établissements d'enseignement et de recherche français ou étrangers, des laboratoires publics ou privés.



Distributed under a Creative Commons Attribution - NonCommercial 4.0 International License

1 Cellulose, proteins, starch and simple carbohydrates molecules  
2 control the hydrogen exchange capacity of bio-indicators and  
3 foodstuffs.

4  
5 A-L. Nivesse<sup>1,2</sup>, N. Baglan<sup>3</sup>, G. Montavon<sup>1</sup>, G. Granger<sup>1</sup>, O. Péron<sup>1\*</sup>  
6

7 <sup>1</sup>SUBATECH, UMR 6457, 4, rue Alfred Kastler, BP 20722, 44307 Nantes Cedex 3, France

8 <sup>2</sup>CEA, DAM, DIF, F-91297 Arpajon, France

9 <sup>3</sup>CEA, DIF, DRF, JACOB, IRCM, SREIT, LRT, F-91297 Arpajon, France

10 [\\*olivier.peron@subatech.in2p3.fr](mailto:olivier.peron@subatech.in2p3.fr)  
11  
12  
13  
14  
15

16 **Keywords:** Organically bound tritium, hydrogen exchangeability, isotopic exchange, buried  
17 tritium.

18  
19  
20 **Highlights:**

- 21 • The buried tritium form was detected in both a bio-indicator (water-milfoil) and a food  
22 chain sample (apple).
- 23 • The content of buried tritium was correlated with the 3D structure level of starch,  
24 cellulose, proteins and simple carbohydrates molecules associations.
- 25 • The key role of the main constituents (starch, cellulose and protein, simple  
26 carbohydrates) in influencing hydrogen exchange capacity was experimentally  
27 demonstrated.
- 28 • The impact of hydrogen exchangeability on the NE-OBT distribution on  
29 environmental matrix constituents was determined.

30

31 **Abstract:**

32 Over the past several years, it has become increasingly acknowledged that Organically Bound  
33 Tritium (OBT) is the most pertinent tritium form for understanding its behavior and  
34 distribution within the biosphere. The fate of tritium actually depends on the accessibility and  
35 exchangeability of hydrogen atoms for isotopic exchanges in natural organic matter,  
36 especially in widespread biomass biomolecules like carbohydrates or proteins. The present  
37 work is therefore aimed at providing a means for improving the knowledge of tritium  
38 speciation and distribution on environmental matrices by evaluating the impact of molecular  
39 structure of various carbohydrate molecules on OBT behavior. We are thus proposing to  
40 assess the exchange capacities of hydrogen from a gas-solid isotopic exchange methodology  
41 in wheat grains, water-milfoil and apple environmental matrices using starch,  
42 cellulose/proteins and simple carbohydrates as their respective main constituents. For wheat  
43 grains, a good agreement was obtained between experimental and theoretical values as a  
44 result of the predominantly simple molecular structure of starch. For both water-milfoil and  
45 apple, the disparities between experimental and theoretical values showed the occurrence of  
46 the buried form of tritium, correlated with the 3D molecular complexity of their main  
47 constituents. The key role played by these determinant constituents on hydrogen exchange  
48 capacity could thus be experimentally demonstrated on several environmental matrices. These  
49 distinct hydrogen exchange capacities were then proven to exert an influence on the NE-OBT  
50 distribution on environmental matrix constituents, in yielding critical information to better the  
51 understanding of tritium distribution and behavior in the environment.

52

## 53 **1. Introduction**

54 At the present time, tritium is one of the main radionuclides released into the environment at  
55 nuclear installations. According to current forecasts, these release rates are expected to rise  
56 due to the planned development of nuclear power plants and their fuel management methods,  
57 as well as to new tritium emitting facilities, such as the International Thermonuclear  
58 Experimental Reactor (ITER) and the Evolutionary Power Reactor (EPR). Understanding the  
59 behavior of tritium in the environment is therefore an ongoing societal issue, in recognizing  
60 this behavior to be directly related to the chemical forms of tritium, i.e. tritium speciation  
61 (ASN, 2010; IRSN, 2017). In environmental matrices, tritium is found in the form of Tissue-  
62 Free Water Tritium (TFWT) and Organically Bound Tritium (OBT) after the integration of  
63 tritiated water (HTO) during photosynthesis and metabolic processes (Diabaté and Strack,  
64 1993; Pointurier *et al.*, 2003). Over the last decade, a focus on monitoring OBT has become a  
65 major concern in many countries for both public and regulatory assurance (Kim *et al.*, 2013;  
66 Péron *et al.*, 2016; Baglan *et al.*, 2018). OBT is typically differentiated into two pools: the  
67 exchangeable pool (E-OBT), which equilibrates with the surrounding atmosphere; and the  
68 non-exchangeable pool (NE-OBT), which is experimentally inert and remains in organic  
69 matter until its degradation (Sepall and Mason, 1961; Kim *et al.*, 2013). The latter is directly  
70 representative of the amount of tritium released into the environment during growth of the  
71 biological organism; the interest of its study lies in the ability to conduct retrospective studies  
72 of tritium release into the environment.

73 From an analytical standpoint, it is widely assumed that the E-OBT fraction corresponds to  
74 the tritium bound to heteroatoms, while the NE-OBT fraction corresponds to the tritium  
75 covalently bound to carbon (Mann, 1971; Kim *et al.*, 2013). Based on the molecular model, it  
76 is then possible to assign to each organic molecule a theoretical exchangeable parameter  
77 ( $\alpha_{model}$ ) from the hydrogen bound to the heteroatom pool versus total hydrogen atoms.

78 However, this description has been challenged since previous studies highlighted major  
79 limitations of E-OBT accessibility in environmental matrices (Sepall and Mason, 1961;  
80 Baumgartner and Donhaerl, 2004; Péron *et al.*, 2018) when comparing the theoretical  
81 ( $\alpha_{model}$ ) parameter to an experimentally determined ( $\alpha_{iso}$ ) parameter (Feng *et al.*, 1993;  
82 Péron *et al.*, 2018). Molecular conformation is thus supposedly responsible for the loss of  
83 exchange capacities from a part of the theoretically exchangeable hydrogen positions, hence  
84 the designation buried tritium (BT) (Baumgartner and Donhaerl, 2004). The IAEA  
85 (International Atomic Energy Agency) has therefore suggested in its EMRAS program  
86 (EMRAS, 2010) that the NE-OBT fraction must be defined as both covalently carbon bound  
87 tritium atoms and buried tritium atoms (Kim *et al.*, 2008; Kim *et al.*, 2013). This issue is still  
88 undergoing heated debate and requires further investigation.

89 The present work is therefore aimed at providing insight into tritium speciation and  
90 distribution on environmental matrices by means of evaluating the impact of molecular  
91 composition and arrangement on OBT behavior. To this end, it is being proposed herein to: (i)  
92 compare ( $\alpha_{model}$ ) and ( $\alpha_{iso}$ ) parameters and, through reliance on the knowledge of  
93 molecular structures, grasp the origin of the buried tritium form, (ii) define the exchangeable  
94 capacity of environmental matrices compared to their main constituent, and (iii) assess the  
95 NE-OBT distribution with respect to both structural and exchangeable aspects.

96 Starch, cellulose, proteins and simple carbohydrates are among the most widespread  
97 biomolecules of the biomass on earth and may be found under diverse molecular structures in  
98 environmental matrices (Sun and Cheng, 2002; Hopkins, 2003; Sakintuna *et al.*, 2003). Two  
99 food chain matrices, i.e. wheat grains and apples, plus a bio-indicator, water-milfoil,  
100 presenting initial anthropogenic OBT activities, have been selected while their main  
101 constituents were effectively extracted in order to represent the corresponding biomolecule  
102 types and undergo exchangeability assessments.

103 To access the exchangeable ( $\alpha_{iso}$ ) parameter, an original methodology based on isotopic  
104 exchange under a soft path regime has been previously developed (Péron *et al.*, 2018) and  
105 subsequently validated for exchange capacity investigations in carbohydrate molecules.  
106 Knowledge of this parameter thus yields insight into the true nature of the exchangeable  
107 hydrogen pool within a studied environmental matrix and serves to improve our  
108 understanding of OBT speciation (Nivesse *et al.*, 2020).

109

110

## 111 **2. Materials and methods**

### 112 **2.1. Reagents and chemicals**

113 Tritium solutions were prepared at the Subatech Laboratory using a certified and calibrated  
114 source and a low-level tritium water source “*Eau des Abatilles*” (whose HTO activity lies  
115 significantly below  $0.2 \text{ Bq.L}^{-1}$  (Fourré *et al.*, 2014)).

116 All reagents were purchased from Fisher Scientific International and met at least ACS reagent  
117 grade (i.e. match or exceed the specifications established by the American Chemical Society).

118 Ultrapure water ( $18.2 \text{ M}\Omega\cdot\text{cm}$  resistivity at  $25^\circ$  and  $< 5 \mu\text{g.L}^{-1}$  TOC) obtained from a Milli-Q  
119 Advantage A10® system (Merck Millipore, France) was used. The tritium contaminations  
120 from reagents were considered to be negligible since the initial tritium activities of the studied  
121 matrices were significantly higher, thus suggesting only tritium depletion could be observed.

### 122 **2.2. Sample preparation**

123 The tritium contents of environmental matrices and extracted constituents were adjusted to the  
124 same reference date of July 1, 2020 by only considering the tritium radioactive decay impact.

125 The initial contents in organically bound tritium (OBT) within environmental matrices and  
126 extracted constituents are recorded in Table 1 (*insert Table 1 here*).

#### 127 *2.2.1. Wheat grains and starch*

128 Wheat grains (Matrix A-1) from the Organically Bound Tritium (OBT) working group were  
129 previously studied as part of the work presented in Péron *et al.* (2018).

130 Starch (Matrix A-2) is the main component of wheat grains (Matrix A-1) and was extracted  
131 according to a procedure adapted from Verwimp *et al.* (2004), Xie *et al.* (2008) and Liu and  
132 Ng (2015). Briefly summarized, wheat flour was obtained from ground and sieved wheat  
133 grains passing through a  $74\text{-}\mu\text{m}$  size sieve. Wheat flour (4 g) was suspended in 28 mL of

134 0.25% (v/v) NaOH, followed by 1 h of stirring prior to 10 min of centrifugation at 3900 x g.  
135 The sediment was then washed three times with deionized water by stirring for 30, 15 and 10  
136 min respectively until final neutralization with 1 M HCl prior to 10 min of centrifugation at  
137 3900 x g for each step. The brown fraction was removed and the white fraction was first  
138 suspended in 15 mL of deionized water then passed through a 75- $\mu$ m nylon screen; approx. 20  
139 mL of deionized water was used to wash the overs. The white extracted starch filtrate was  
140 freeze-dried for 1 week and stored under vacuum prior to further use.

#### 141 2.2.2. *Water-milfoil and the cellulosic wall*

142 Water-milfoil (Matrix B-1) samples were taken from the Loire River (47°45'18.7"N,  
143 2°28'25.3"E) 2 km downstream of the Dampierre Nuclear Power Plant (NPP) (France). The  
144 fresh samples were immediately transferred into sealed plastic bags and stored frozen. After  
145 48 h of freezing, the samples were dehydrated by oven drying at 90°C for 2 weeks. Freeze-  
146 drying was performed for 48 h to ensure complete removal of the free water fraction, and  
147 lastly the samples were stored under vacuum.

148 The cellulosic wall (Matrix B-2) of water-milfoil (Matrix B-1) was recovered by extraction  
149 and elimination of the cytoplasmic fraction following a procedure adapted from Sun *et al.*  
150 (2004) and Mochochoko *et al.* (2013). Briefly summarized, freeze-dried water-milfoil were  
151 ground to pass a 1-mm size sieve, and the resultant powder (100 g) was dewaxed with  
152 toluene-ethanol (2:1 v/v) in a Soxhlet apparatus at 80°C for 6 h, followed by filtration at 63  
153  $\mu$ m and washing with ethanol (96% v/v) for 24 h. Extra washing steps with water and ethanol  
154 (96% v/v) were carried out to ensure a high degree of purification. The gradual loss of green  
155 coloration was due to chloroplast leak and representative of the effective removal of the  
156 cytoplasmic fraction. The purified powder was then allowed to dry in an oven at 90°C for 48  
157 h, freeze-dried for 48 h and stored under vacuum.

158



159 2.2.3. *Apples and simple carbohydrates*

160 Apples (Matrix C-1) were sampled at a distance 2 km from the Cernavodă Nuclear Power  
161 Plant (NPP) (Romania, 44°20'10.0"N 28°02'13.9"E). Fresh samples were roughly cut and  
162 stored frozen for 48 h, then freeze-dried for 2 weeks, ground to pass a 1-mm size sieve and  
163 stored under vacuum.

164 Simple carbohydrates (Matrix C-2) were extracted from the apples (Matrix C-1) according to  
165 the procedure described in Besle and Pitiot (1976). Briefly summarized, apples were cut into  
166 thin strips, and the resultant sample (20g) was extracted with 1 L ethanol (85% v/v) under  
167 reflux and stirring at 80°C for 1 h. After successive filtrations at 63, 20 and 0.45 µm with  
168 manufactured filters, the extracted solution was reduced using Rotavapor concentration and  
169 then freeze-dried for 1 week, homogenized under dried atmosphere (RH < 10%) and stored  
170 under vacuum.

171

172 **2.3. Sample characterization**

173 The samples were characterized on each studied matrix, and the composition in % by weight  
174 was recorded. A broad range of common components was investigated, with certain  
175 components being examined more closely by virtue of representing the specific constituents  
176 of selected matrices. The common components tested were: starch, cellulose, sucrose,  
177 proteins, and fat contents. For starch-type matrices, i.e. A-1 and A-2, the main essential amino  
178 acids of the former were described in Péron *et al.* (2018), while the maltose and glucose  
179 contents were determined in the latter by applying the AACC 76-13.01 Standard method with  
180 the Total StarchKit Assay (Megazyme International Ireland Ltd. Co., Wicklow, Ireland). For  
181 cellulose-type matrices, i.e. B-1 and B-2, the proportions in parietal constituents of cellulose,  
182 hemicellulose and lignin were analyzed using NDF (neutral detergent fiber), ADF (acid

183 detergent fiber) and ADL (acid detergent lignin) analyses, as stated in Van Soest (1963). For  
184 simple carbohydrate-type matrices, i.e. C-1 and C-2, the fructose and glucose contents were  
185 also recorded.

186 For each previously analyzed component, a theoretical exchangeable parameter ( $\alpha_{model}$ ) was  
187 calculated from their respective literature-based and well-known molecular formula according  
188 to the analytical definition of E-OBT, i.e. hydrogen bound heteroatoms are exchangeable  
189 hydrogen. On this basis, a theoretical exchangeable parameter ( $\alpha_{model}$ ) could then be  
190 calculated for each matrix according to its composition in % by weight in each component  
191 and its assigned unitary ( $\alpha_{model}$ ). The contribution of the mineral fraction was considered to  
192 be negligible due to the low hydrogen content found in the mineral fractions of living organic  
193 matrices.

194

#### 195 **2.4. Isotopic exchange procedure**

196 The gas-solid isotopic exchange process, as described in Péron *et al.* (2018), is based on the  
197 isotopic steady state between a bath of KCl-saturated solution ( $\left(\frac{T}{H}\right)_{l, bath}$ ), a vapor phase  
198 confined in a glove box ( $\left(\frac{T}{H}\right)_{g, vapor}$ ), the water condensed at the sample surface ( $\left(\frac{T}{H}\right)_{l, cond}$ )  
199 and the exchangeable organically bound tritium of the sample ( $\left(\frac{T}{H}\right)_{s, E-OBT}$ ), as set forth in  
200 Eq. (1):

$$\left(\frac{T}{H}\right)_{l, bath} = \left(\frac{T}{H}\right)_{g, vapor} = \left(\frac{T}{H}\right)_{l, cond} = \left(\frac{T}{H}\right)_{s, E-OBT} \quad (1)$$

201

202 As part of this description, a vapor phase has been produced from a bath containing saturated  
203 KCl solutions with controlled tritium activities, for the purpose of equilibration with the

204 atmosphere contained in a glove box ( $RH = 85.11 \pm 0.89\%$  at  $T = 20^\circ\text{C}$ , Plas-Labs 890-THC)  
205 (see Péron *et al.* (2018) for further details).

206  
207 Isotopic exchanges were separately conducted on each studied matrix following both one  
208 tritium-depletion experiment with a low-level tritium bath ( $\text{HTO} < 0.2 \text{ Bq.L}^{-1}$ ) and three  
209 tritium-enrichment experiments with tritium-rich baths ( $\text{HTO} = 120, 300 \text{ and } 500 \text{ Bq.L}^{-1}$ ).  
210 Three aliquots were extracted from each bath during the isotopic exchange step to quantify  
211 the exact HTO activity. Samples were recovered from the confined glove box at days 2, 3 and  
212 4 to ensure that steady state had been reached. After liquid nitrogen immersion and freeze-  
213 drying, the samples were heat-treated in a tubular furnace (Eraly, France), where the organic  
214 matter was transformed into carbon dioxide and combustion water (Cossonnet *et al.*, 2009;  
215 CETAMA, 2013; Péron *et al.*, 2016). Bath aliquots and combustion water from the samples  
216 were distilled and neutralized for pH correction, if needed, while tritium activities were  
217 measured by means of liquid scintillation counting (PerkinElmer Tri-carb 3170 TR/SL) using  
218 an Ultima Gold LLT cocktail. The detection limit was estimated at  $3 \text{ Bq.L}^{-1}$  for a counting  
219 time of 180 minutes and a blank value of 2 counts per minute. The relative uncertainty was  
220 calculated based on a calibration step, according to the quench curve and systematic  
221 uncertainties; this relative uncertainty typically reached 10%.

222  
223 At each steady state, a mean value of the combustion water from each matrix sample  
224  $\left(\frac{T}{H}\right)_{s, OBT}$  was obtained by averaging the sample values forming the plateau. A mean value of  
225 each saline solution  $\left(\frac{T}{H}\right)_{l, bath}$  was also derived by averaging the three bath aliquot values  
226 once steady state had been reached.

## 227 **3. Results**

### 228 **3.1. Molecular model-based theoretical exchangeable parameter ( $\alpha_{model}$ )**

229 For each studied matrix, a theoretical exchangeable parameter ( $\alpha_{model}$ ) was calculated from  
230 the molecular model of its main components and respective experimentally determined  
231 composition in % by weight. The main essential components analyzed along with their  
232 associated ( $\alpha_{model}$ ) and distributions in % by weight in the A-1, A-2, B-1, B-2, C-1 and C-2  
233 matrices are listed in Table 2 (*insert Table 2 here*). The distribution in % by weight of starch  
234 (A-2) in wheat grains (A-1) was directly measured at  $75.3 \pm 3.7\%$  of organic matter. Towards  
235 the cellulosic wall (B-2) in water-milfoil, this distribution was estimated at  $56 \pm 27\%$  of  
236 organic matter by assuming that the entire cellulose, hemicellulose and lignin parts were  
237 recovered ( $40.6 \pm 7.3\%$  in water-milfoil) and moreover that the protein fraction found in the  
238 cellulosic wall was correlated with the structural proteins part without the cytoplasmic  
239 proteins part (calculated at  $15.2 \pm 6.8\%$  and  $22.1 \pm 9.6\%$  in water-milfoil, respectively). For  
240 simple carbohydrates (C-2), their distribution in % by weight of organic matter was calculated  
241 at  $88.2 \pm 5.9\%$  in apple (C-2) due to the addition of its respective content in glucose, sucrose  
242 and fructose. The resultant calculated ( $\alpha_{model}$ ) parameters on each studied matrix are given  
243 in Table 3.

244 Starch and cellulose are two of the most abundant bio-macromolecules of terrestrial  
245 ecosystems. They are carbohydrate molecules of glucose monomer ( $(C_6H_{10}O_5)_n$ ) with 3/10  
246 hydrogen atoms bound to hydroxyl groups, hence an assigned ( $\alpha_{model}$ ) equal to 30% was  
247 adopted for these polysaccharides. Glucose and fructose are simple carbohydrate monomer  
248 molecules ( $C_6H_{12}O_6$ ) with 5/12 hydrogen atoms bound to hydroxyl groups, explaining the  
249 assigned ( $\alpha_{model}$ ) value of 41.7%. Maltose, composed of two glucose molecules, and sucrose,

250 comprising one molecule of glucose and one of fructose, are simple carbohydrates with an  
251 assigned ( $\alpha_{model}$ ) value of 36.4%.

252 Lignin is a macromolecule composed of variable polyphenolic polymer biomolecules, whose  
253 structure and organization depend on the environmental physicochemical conditions of  
254 formation. Lignin is mainly found with an association of proportional coumaryl, coniferyl and  
255 sinapyl alcohols (Kratzl *et al.*, 1976) with ( $\alpha_{model}$ ) equal to 20, 18.2 and 15.4%, respectively.  
256 Considering that the loss in hydrogen atoms bound to carbon and those bound to hydrogen  
257 compensates for each unit bond, as identified in several theoretical molecular structures and  
258 conformations of this biomolecule (Hopkins, 2003), the ( $\alpha_{model}$ ) value assigned to lignin was  
259 estimated at 17%.

260 Hemicellulose is a cellulose-like macromolecule predominantly represented in the dual form  
261 of xyloglucan ( $(\alpha_{model}) = 29.2\%$ ) and arabinoxylan ( $(\alpha_{model}) = 25\%$ ) (Hopkins, 2003) in  
262 primary and secondary plant cell walls. In order to maintain the representativeness of these  
263 two biomolecules, the ( $\alpha_{model}$ ) value assigned to hemicellulose was estimated at 27.1% for  
264 our study.

265 Protein content was determined by means of total nitrogenous content quantification. Proteins  
266 are made up of amino acids whose ( $\alpha_{model}$ ) values lie within a range of 23 to 58%. The  
267 essential amino acids were therefore analyzed in each matrix separately. For matrix A-1, the  
268 composition in % by weight is available in Péron *et al.* (2018) and the ( $\alpha_{model}$ ) for proteins  
269 was calculated at 37%. For matrices B-1 and B-2, the amino acid composition was determined  
270 by data available in the literature (Muztar *et al.*, 1978) and an assigned ( $\alpha_{model}$ ) for proteins  
271 of 42% was estimated. For the A-2, C-1 and C-2 matrices, the protein content was considered  
272 to be negligible.

273 Fat molecules primarily consist of carbon and hydrogen atoms with a highly negligible  
274 amount of hydrogen atoms bound to the heteroatom representation (Péron *et al.*, 2018). The  
275 ( $\alpha_{model}$ ) assigned to fat molecules is thus less than 0.1% but must still be considered when  
276 performing calculations.

277

### 278 **3.2. Isotopic exchange-based exchangeable parameter ( $\alpha_{iso}$ )**

279 Isotopic exchanges were conducted on each studied matrix with various T/H ratios in order to  
280 evaluate the isotopic exchangeable parameter ( $\alpha_{iso}$ ), as described in Péron *et al.* (2018).

281 For each steady state achieved, the mean value of the combustion water from each matrix  
282 sample  $\left(\frac{T}{H}\right)_{s, OBT}$  was plotted versus the mean value of each saline solution  $\left(\frac{T}{H}\right)_{l, bath}$ , as  
283 presented for each matrix in Figure 1 (*insert Figure 1 here*). The slope of the linear regression  
284 obtained was therefore considered as ( $\alpha_{iso}$ ) and calculated according to Eq. (2):

$$\alpha_{iso} = \frac{\Delta\left(\frac{T}{H}\right)_{s, OBT}}{\Delta\left(\frac{T}{H}\right)_{l, bath}} \quad (2)$$

285 From this set-up, a wide range of isotopic exchangeable parameters ( $\alpha_{iso}$ ) was obtained on  
286 the studied environmental matrices, i.e. from  $16.1 \pm 0.6\%$  to  $39.6 \pm 1.3\%$ , and compared to  
287 the ( $\alpha_{model}$ ) listed in Table 3 (*insert Table 3 here*). The standard uncertainties on ( $\alpha_{iso}$ )  
288 parameters were calculated using the least squares method with a coverage factor k equal to 2.

289

### 290 **3.3. Determination of the non-exchangeable organically bound tritium (NE-OBT)**

291 Following the isotopic depletion exchange experiment, which was conducted separately on  
292 each studied matrix with a low-level tritium bath ( $HTO < 0.2 \text{ Bq.L}^{-1}$ ), the samples were  
293 devoid of exchangeable organically bound tritium (E-OBT) atoms. The remaining tritium

294 fraction at steady state thus relates to the non-exchangeable organically bound fraction (NE-  
 295 OBT). After an adequate post-treatment, as previously described, the activities measured in  
 296 the combustion waters of the three solid sample replicates were averaged to obtain a mean  
 297 NE-OBT value in each analyzed matrix.

298 Furthermore, supplementary information provided by the gas-solid isotopic exchange process  
 299 served to calculate  $\left(\frac{T}{H}\right)_{s, NE-OBT}$  by using Eq. (3) (Péron *et al.*, 2018) obtained below:

$$\left(\frac{T}{H}\right)_{s, NE-OBT} = \frac{\left[\left(\frac{T}{H}\right)_{s, OBT} - \alpha_{iso} \times \left(\frac{T}{H}\right)_{l,bath}\right]}{(1 - \alpha_{iso})} \quad (3)$$

300

301 The results produced, expressed in Bq.L<sup>-1</sup> of combustion water (NE-OBT (Bq.L<sup>-1</sup>)), were  
 302 converted into Bq.kg<sup>-1</sup> of dry matter (NE-OBT (Bq.kg<sup>-1</sup>)) using the content in % by weight of  
 303 hydrogen in each matrix (%H<sub>ech</sub>) as well as that in water (%H<sub>water</sub>) by applying Eq. (4)  
 304 below:

305

$$NE - OBT (Bq. kg^{-1}) = NE - OBT (Bq. L^{-1}) \times \frac{\%H_{sample}}{\%H_{water}} \quad (4)$$

306

307 The measured and calculated values of NE-OBT for each studied matrix are presented in  
 308 Table 4 (*insert Table 4 here*). The uncertainties associated with the results obtained were  
 309 determined by calculating the average uncertainty and the propagation of uncertainties  
 310 squared using a coverage factor k equal to 2. For each matrix, these two values were similar  
 311 and displayed consistent assigned values of relative uncertainties. Accordingly, only the  
 312 measured values will be mentioned in the Discussion section.

313

## 314 4. Discussion

### 315 4.1. The impact of molecular structure on hydrogen exchangeability

316 Among all the matrices studied, only wheat grains (Matrix A-1) and their extracted starch  
317 (Matrix A-2) presented both isotopic exchangeable parameter results ( $\alpha_{iso}$ ) =  $31.0 \pm 1.0\%$   
318 and ( $\alpha_{iso}$ ) =  $31.1 \pm 1.0\%$ , respectively) similar to their calculated theoretical exchangeable  
319 parameters ( $\alpha_{model}$ ) =  $30.0\%$  and ( $\alpha_{model}$ ) =  $31.6\%$ , respectively). Wheat grains are mainly  
320 composed of starch, a macromolecule comprising 25% amylose ( $\alpha(1\rightarrow4)$  bound glucose  
321 molecules) and 75% amylopectin ( $\alpha(1\rightarrow4)$  bound glucose molecules branched with  $\alpha(1\rightarrow6)$   
322 bound glucose molecules) (Sakintuna *et al.*, 2003). These glucose polymers exhibit well-  
323 known linear and helical molecular structures with a predominantly weak crystalline area and  
324 only a few intermolecular hydrogen bonds (Tester *et al.*, 2004). It can then be assumed that  
325 the analytical point of view (i.e. based on chemical bond type) is well suited and adequate to  
326 describe OBT speciation and behavior for this specific type of environmental matrix  
327 molecular structure.

328  
329 In contrast, results obtained on the other matrices studied (B-1 and C-1) showed disparities  
330 between the calculated exchangeable parameter ( $\alpha_{model}$ ) and the isotopic exchangeable  
331 parameter ( $\alpha_{iso}$ ) obtained from the vapor phase (T/H) isotopic exchange experiment.  
332 According to the state-of-the-art, the first hypothesis implies that this difference is correlated  
333 with the presence of buried tritium due to the explanation of the exchangeability phenomenon  
334 inertia derived from the local 3D structure. For this reason, such compounds are particularly  
335 prized.

336  
337 Water-milfoil (Matrix B-1) yielded an isotopic exchangeable parameter ( $\alpha_{iso}$ ) =  $26.4 \pm$   
338  $0.5\%$ ) below the calculated theoretical exchangeable parameter ( $\alpha_{model}$ ) =  $31.5\%$ ). This



339 matrix is mainly composed of starch, proteins and cellulosic compounds (cellulose,  
340 hemicellulose and lignin), but only the last two are capable of presenting complex 3D  
341 molecular structures. Let's start out discussion with cellulose since it contains a long linear  
342 unbranched chain of D-glucose units linked through  $\beta(1\rightarrow4)$ -glycosidic bonds with monomer  
343 arrangements oriented at  $180^\circ$ , thus promoting the formation of both intra and intermolecular  
344 hydrogen bonds and allowing for the distinction of amorphous and crystalline regions  
345 (Zugenmaier, 2001; Klemm *et al.*, 2005; Wuestenberg, 2014). This specific structural  
346 stabilization corresponds to a three-dimensional network (Nishiyama *et al.*, 2003, 2002;  
347 Jarvis, 2003), whose involvement in decreasing hydrogen exchangeability has already been  
348 discussed in Péron *et al.* (2018). In this 2018 investigative work, isotopic exchangeable  
349 parameters ( $\alpha_{iso}$ ) were observed at  $13.0 \pm 1.0\%$  and  $21.0 \pm 1.0\%$  in commercial celluloses  
350 with various crystalline ratios (with respect to ( $\alpha_{model}$ ) = 30%). The hydrogen bond  
351 phenomenon present in the crystalline regions of celluloses therefore justifies that a portion of  
352 hydrogen atoms in the theoretical exchangeable position could behave as if they were placed  
353 in non-exchangeable positions.

354 Such a phenomenon can also be expected with proteins possessing a three-dimensional  
355 structure. Proteins are in fact polypeptides of amino acids linked by peptide bonds occurring  
356 between a carboxyl group and an amine function (Richardson, 1981; Makhatadze and  
357 Privalov, 1995; Kim *et al.*, 2008). Each peptide bond formation thus leads to the elimination  
358 of two theoretically exchangeable hydrogen atoms from the initial molecule of two amino  
359 acid units. The three-dimensional protein structures are then defined by a pattern of hydrogen  
360 bonds between these primary chain peptide groups, with a regular geometry of mostly  $\alpha$ -helix  
361 and  $\beta$ -sheet saturating all the hydrogen bond donors and acceptors in the peptide backbone  
362 (Richards, 1977; Branden and Tooze, 2012; Shulz and Schirmer, 2013). These aspects of the  
363 protein structure are then more likely to induce a drastic impact on the exchangeable

364 parameter of the entire protein chain, depending on the sequence length and nature of the  
365 amino acid units involved.

366 As such, the cellulosic wall (Matrix B-2) containing all the resultant cellulosic compounds  
367 along with a portion of the proteins (the structural proteins part) were recovered from the  
368 water-milfoil. After the compositional analyses and isotopic exchange process, a considerable  
369 gap was observed between this cellulosic wall theoretical exchangeable parameter  
370 ( $(\alpha_{model}) = 29.0\%$ ) and its corresponding isotopic exchangeable parameter ( $(\alpha_{iso}) = 16.1 \pm$   
371  $0.6\%$ ). These elements therefore enable corroborating the hypothesis of a massive impact of  
372 the cellulose and protein compounds found in environmental matrix structures on hydrogen  
373 exchangeability, i.e. the presence of crystalline parts and then three-dimensional local  
374 structures yields buried tritium.

375  
376 The apples (Matrix C-1) also presented an isotopic exchangeable parameter ( $(\alpha_{iso}) = 28.0 \pm$   
377  $1.7\%$ ) significantly below the corresponding calculated theoretical exchangeable parameter  
378 ( $(\alpha_{model}) = 38.7\%$ ). This matrix is basically composed of simple carbohydrates displaying a  
379 very high theoretical exchangeability rate, with an assigned ( $\alpha_{model}$ ) value of up to 41.7%  
380 (see Table 2). However, simple carbohydrates are known to partially adopt a specific  
381 conformation in complex environmental matrices and form compact aggregates with crystal  
382 or ramified arrangements (Beevers *et al.*, 1952; Kanters *et al.*, 1977). As previously noted for  
383 water-milfoil (Matrix B-1), these crystalline regions, which are typically characterized by a  
384 hydrogen bond, may supposedly be responsible for the observed decrease of hydrogen  
385 exchangeability in apples. Ramified arrangements of sugars in environmental matrices are  
386 also assumed to contain a hydrogen bond and favor a structure hindering phenomenon that  
387 could explain the loss in hydrogen exchangeability as well.

388 To confirm this hypothesis, simple carbohydrates (Matrix C-2) were extracted from apples  
389 and underwent partial destruction of their initial complex 3D structure due to solubilization  
390 during the extraction process. The polar nature of simple carbohydrate molecules does indeed  
391 provide them with both a property of very high solubility in water; moreover, access to a  
392 substantial amount of water during the extraction process was assumed to allow for their  
393 entire solubilization and dissociation from other simple carbohydrate associations (Lee *et al.*,  
394 2011). It is important to note that, as opposed to other previously extracted component  
395 matrices (i.e. A-2 and B-2 from A-1 and B-1) with a preserved initial structure, the simple  
396 carbohydrate matrix (C-2) extraction process from Matrix C-1 was intended to trigger  
397 destruction of the initial sugar structure arrangements due to solubilization. After  
398 compositional analyses and the isotopic exchange process, the extracted matrix (C-2)  
399 presented theoretical and experimental values closely bunched together as compared to the  
400 raw (C-1) matrix, i.e. ( $\alpha_{model}$ ) = 40.4%) versus ( $\alpha_{iso}$ ) =  $39.6 \pm 1.3\%$ ). These results have  
401 shown that the molecular conformation destruction of sugars leads to the opening of their  
402 initial ramified structure, thus allowing the entire pool of theoretically exchangeable hydrogen  
403 atoms to be accessible for isotopic exchange with the surrounding atmosphere. As such, it can  
404 be assumed that the initial complex 3D structure of simple carbohydrates (Matrix C-2) in  
405 apples (Matrix C-1) is responsible for the hindering phenomenon and hence for the  
406 inaccessibility of a portion of the theoretically exchangeable hydrogen atoms in sugar-like  
407 environmental matrices.

408

409 Whenever environmental matrices are composed of various compounds with an array of  
410 complex 3D molecular conformations, such as a crystalline structure or ramified arrangement,  
411 it then becomes possible to ensure that the analytical point of view (i.e. based on chemical  
412 bond type) is insufficient to describe OBT speciation and behavior. In contrast, the molecules

413 displaying a simple molecular conformation and arrangement like starch do not appear to  
414 cause buried tritium forms in wheat grains, which allows confirming that the analytical point  
415 of view is indeed sufficient to describe the NE-OBT and E-OBT forms on starch-like  
416 environmental matrices. The inferiority or equality observed between the isotopic  
417 exchangeable parameter ( $\alpha_{iso}$ ) and the theoretical parameter ( $\alpha_{model}$ ) have therefore  
418 highlighted the relatively substantial presence or total absence of the buried tritium (BT) form  
419 depending on the molecular structure specificities and complexity of the studied  
420 environmental matrices and their main component.

421

## 422 **4.2. Exchangeable capacity of environmental matrices and impact of NE-OBT**

### 423 **distribution**

424 The isotopic exchange results on extracted matrices A-2, B-2 and C-2 revealed that the  
425 structure of their constituents has exerted an influence on the global behavior of hydrogen in  
426 environmental matrices A-1, B-1 and C-1. Considering the distribution of starch (A-2) in %  
427 by weight in wheat grains (A-1) (i.e.  $75.3 \pm 3.7\%$ ) and the distribution of the cellulosic wall  
428 (B-2) in % by weight in water-milfoil (B-1) (i.e.  $56 \pm 27\%$ ), as provided in Table 4, it then  
429 appears that the isotopic exchangeable parameters ( $\alpha_{iso}$ ) of the extracted matrices directly  
430 predetermine that of the environmental matrices being studied (Table 3). The result obtained  
431 on the B-2 matrix ( $\alpha_{iso}$ ) =  $16.1 \pm 0.6\%$  and the ( $\alpha_{model}$ ) of the other constituents associated  
432 with their weight distribution in B-1 would actually lead to results calculated on the  
433 exchangeability parameter ( $\alpha_{iso_{calculated}}$ ) for the B-1 matrix very close to the results obtained  
434 by isotopic exchange (approx.  $24.2 \pm 14.9\%$  vs. an actual of  $26.4 \pm 0.5\%$ ). From this finding,  
435 a slight relative difference ( $\alpha_{iso_{calculated}}$  deviation) of  $8 \pm 5\%$  was recorded from this  
436 calculated exchangeability parameter ( $\alpha_{iso_{calculated}}$ ) compared to the experimental ( $\alpha_{iso}$ )

437 parameter on the B-1 matrix. In the case of matrices A-1 and A-2, both ( $\alpha_{iso}$ ) results were  
 438 also basically equal, which exhibits the exchangeability rate control from the extracted main  
 439 components. The relative difference of ( $\alpha_{iso}$ ) vs. a calculated exchangeability parameter  
 440 ( $\alpha_{iso_{calculated}}$ ) (approx.  $31.1 \pm 0.8\%$ ) was then determined to equal  $0.4 \pm 0.1\%$ . Regarding the  
 441 apple (C-1) and simple carbohydrate (C-2) matrices, the significant difference ( $\alpha_{iso_{calculated}}$   
 442 deviation) of  $26 \pm 7\%$  between the two parameters was directly explained by the inherent  
 443 partial degradation and modification of the initial structure of simple carbohydrates during the  
 444 extraction process. The extracted simple carbohydrate (C-2) molecular structure was indeed  
 445 no longer representative of the initial structure inside the apple (C-1) matrix, thus preventing  
 446 any establishment of a direct link between the two matrices and their respective  
 447 exchangeability parameters.

448 From the results with starch (A-2) and cellulosic wall (B-2) as the major and determinant  
 449 constituents for hydrogen exchangeability in wheat grains (A-1) and water-milfoil (B-1)  
 450 respectively, an exchangeable capacity model of hydrogen in environmental matrices can then  
 451 be expressed by the following formula:

$$(\alpha_{iso_{calculated}_X}) = \sum r_{x_{i-det}} \times (\alpha_{iso})_{x_{i-det}} + r_{x_i} \times (\alpha_{model})_{x_i} \quad (7)$$

452 where:

453 ( $\alpha_{iso_{calculated}}$ ) = the calculated isotopic exchangeable parameter of environmental matrix  
 454 “X”,

455  $r_{x_{i-det}}$  = the distribution in % by weight of the determinant constituent “ $x_{i-det}$ ” of the matrix,

456 ( $\alpha_{iso}$ ) $_{x_{i-det}}$  = its isotopic exchangeable parameter,

457  $r_{x_i}$  = the distribution in % by weight of every other “x” constituent of matrix “X”,

458  $(\alpha_{iso})_{x_i}$  = the isotopic exchangeable parameter of every other “x” constituent of matrix “X”.

459

460 The deviations between calculated ( $\alpha_{iso\text{calculated}}$ ) parameters and experimental ( $\alpha_{iso}$ )  
461 parameters for each of the studied environmental matrices are reported in Table 3. The  
462 determinant constituent  $x_{i-det}$  of an environmental matrix is then designated not only as one  
463 of the main constituents but also with specific structural arrangements in the particular  
464 environmental matrix.

465

466 Furthermore, the calculated distributions of the initial NE-OBT matrix on the determinant  
467 extracted matrix in our present study (Table 4) would seem to display a relative trend  
468 proportional to the mass distribution of the given compounds while also undergoing influence  
469 from their isotopic exchangeable parameter ( $\alpha_{iso}$ ).

470 A NE-OBT recovery rate on the cellulosic wall (B-2) from water-milfoil (B-1) of  $44 \pm 22\%$   
471 was thus observed with a slight downward trend for its own mass distribution in the initial  
472 matrix, i.e.  $56 \pm 27\%$ , thus suggesting the hypothesis that a smaller portion of the non-  
473 exchangeable organically bound tritium (NE-OBT) might be located in this area rather than  
474 other compounds. In displaying the lowest ( $\alpha_{iso}$ ) parameter value due to crystalline and local  
475 three-dimensional structures of cellulose and proteins, the cellulosic wall (B-2) is potentially  
476 subjected to a slight tritium distribution deprivation during molecular synthesis and sample  
477 growth as a result of the 3D molecular complexity of these compounds. On the other hand, the  
478 NE-OBT recovery rate on A-2 from A-1 of  $71.0 \pm 8.7\%$  appears to conform to the mass  
479 distribution of the constituent ( $75.3 \pm 3.7\%$ ), demonstrating that the exchangeability rate  
480 concordance of these two matrices leads to a proportional mass distribution of the NE-OBT  
481 on the raw matrix (A-1). Concerning apples (C-1) and their simple carbohydrates (C-2), the  
482 structural modification of sugars during the extraction step was assumed to be responsible for

483 opening the ramified structure, hence leading to the accessibility of a pool of theoretically  
484 hindered exchangeable hydrogen atoms, as translated by a higher value obtained for the  
485 ( $\alpha_{iso}$ ) parameter. This phenomenon has been confirmed by the extremely low NE-OBT  
486 recovery rate onto C-2 from C-1 (i.e.  $47 \pm 11\%$  of recovery rate vs. a weight distribution of  
487  $88.2 \pm 5.9\%$ ), since part of the measured NE-OBT on apple (C-1) was actually buried tritium  
488 (hindered tritium form) and freed during the molecular structure modification of simple  
489 carbohydrates (C-2). Consequently, this freed buried tritium recovered its exchangeability  
490 capacities and behaved like E-OBT, thus ultimately leading to a lower value of NE-OBT  
491 measured after isotopic exchange depletion in simple carbohydrates (C-2) compared to their  
492 mass distribution in C-1.

493 It is therefore possible to affirm that the hydrogen exchangeability behavior of an  
494 environmental matrix is controlled and established by one of its determinant constituents,  
495 which implies a proven influence on the OBT distribution on environmental matrices.

496

## 497 **5. Conclusion**

498 The impact of molecular structure and conformation on tritium behavior has been highlighted  
499 and evaluated in both food chain and bio-indicator matrices, as well as in widespread  
500 biomolecules contained in the Earth's biomass. Theoretical ( $\alpha_{model}$ ) parameters were  
501 compared to experimentally determined ( $\alpha_{iso}$ ) parameters to understand OBT speciation of  
502 studied matrices in respect to their molecular constituent. Complex 3D molecular structures of  
503 cellulose, proteins and simple carbohydrates have been identified as responsible for the  
504 hydrogen exchangeability decrease in the water-milfoil and apple matrices. The presence of  
505 the buried tritium form was thus detected for environmental matrices containing main  
506 constituents with crystalline structures or ramified molecular arrangements, while its non-  
507 appearance was concluded in wheat grains and correlated with the simpler structure of the  
508 starch molecule. It has thus been shown that determinant constituents with specific molecular  
509 conformation have total control over the hydrogen transfer mechanisms in environmental  
510 matrices and directly establish their associated exchangeable hydrogen capacity. OBT  
511 speciation in a matrix was then found to be entirely correlated to OBT speciation in its  
512 determinant constituent. A significant influence of these structural aspects was observed on  
513 the NE-OBT distribution in environmental matrix constituents, hence providing access to  
514 critical information on remnant tritium in organic matter and tritium transfer in the  
515 environment.

516

## 517 **Acknowledgments**

518 This work was financed by the CEA Research Center, Subatech Laboratory, France's Loire  
519 Valley Regional Council (under the POLLUSOLS OSUNA Project) and the EDF utility  
520 company. The authors would also like to thank the members of the Environmental Laboratory



521 at the Cernavodă Nuclear Power Plant for providing the apple matrix and Gurban Rousseau  
522 from SMART Nantes laboratories for supervising water-milfoil matrix sampling.  
523

## 524 **References**

- 525 ASN, 2010. Le livre blanc du tritium, groupes de réflexion menés de mai 2008 à avril 2010  
526 sous l'égide de l'ASN.
- 527 Baglan, N., Cossonnet, C., Roche, E., Kim, S.B., Croudace, I., Warwick, P., 2018. Feedback  
528 of the third interlaboratory exercise organised on wheat in the framework of the OBT  
529 working group. *J. Environ. Radioact.* Vol. 181(1), 52–61.
- 530 Baumgartner, F., Donhaerl, W., 2004. Non-exchangeable organically bound tritium (OBT): its  
531 real nature. *Anal. Bioanal. Chem.* Vol. 379(2), 204–209.
- 532 Beevers, C.A., McDonald, T.R.R., Robertson, J.T., Stern, F., 1952. The crystal structure of  
533 sucrose. *Acta Crystallogr.* Vol. 5(5), 689–690.
- 534 Besle, J.M., Pitiot, M., 1976. Extraction et purification des glucides: application à divers  
535 aliments dérivés du soja. *Ann. Biol. Anim. Biochim. Biophys.* Vol. 16(5), 753–772.
- 536 Branden, C.I., Tooze, J., 2012. Introduction to protein structure. Garland Sci.
- 537 CETAMA, 2013. Analyse des radionucléides dans l'environnement - Analyse du tritium dans  
538 les matrices, méthode 384. Note Tech. CETAMA.
- 539 Cossonnet, C., Neiva Marques, A.M., Gurriaran, R., 2009. Experience acquired on  
540 environmental sample combustion for organically bound tritium measurement. *Appl.*  
541 *Radiat. Isot.* Vol. 67(5), 809–811.
- 542 Diabaté, S., Strack, S., 1993. Organically bound tritium. *Health Phys.* Vol. 65(6), 698–712.
- 543 EMRAS, 2010. EMRAS (Environmental Modelling of Radiological Safety) Program,  
544 Modelling the Environmental Transfer of Tritium and Carbon-14 to Biota and Man.  
545 Final Report. Tritium and Carbon-14 Working Group. IAEA Vienna Austria.
- 546 Feng, X., Krishnamurty, R.V., Epstein, S., 1993. Determination of D/H ratios of  
547 nonexchangeable hydrogen in cellulose: a method based on the cellulose-water  
548 exchange reaction. *Geochem Cosmochim Acta* Vol. 57, 4249–4256.

549 Fourré, E., Jean-Baptiste, P., Dapoigny, A., Ansoborlo, E., & Baglan, N. 2014. “Reference  
550 waters” in French laboratories involved in tritium monitoring: how tritium-free are  
551 they?. *Radioprotection*, Vol. 49(2), 143-145.

552 Hopkins, W.G., 2003. *Physiologie végétale*. Ed. Boeck Supér.

553 IRSN, 2017. *Rapport Actualisation des connaissances Tritium Environnement*. Ed. Inst.  
554 Radioprot. Sûreté Nucl. IRSN.

555 Jarvis, M., 2003. Chemistry: cellulose stacks up. *Nature* Vol. 426, 611–612.

556 Kanters, J.A., Roelofsen, G., Alblas, B.P., Meinders, I., 1977. The crystal and molecular  
557 structure of  $\beta$ -d-fructose, with emphasis on anomeric effect and hydrogen-bond  
558 interactions. *Acta Crystallogr. B* Vol. 33(3), 665–672.

559 Kim, S.B., Baglan, N., Davis, P.A., 2013. Current understanding of organically bound tritium  
560 (OBT) in the environment. *J. Environ. Radioact.* Vol. 126(1), 83–91.

561 Kim, S.B., Workman, W.J.G., Davis, P.A. (2008) Experimental investigation of buried  
562 tritium in plant and animal tissues, *Fusion Science and Technology*, Vol. 54, 257-260.

563 Klemm, D., Heublein, B., Fink, H.-P., Bohn, A., 2005. Cellulose: Fascinating Biopolymer and  
564 Sustainable Raw Material. *Angew. Chem. Int. Ed.* Vol. 44(22), 3358–3393.

565 Kratzl, K., Claus, P., Reichel, G., 1976. Reactions of lignin and lignin model compounds with  
566 ozone. *Tappi* Vol. 59(11), 86–87.

567 Lee, J.W., Thomas, L.C., Schmidt, S.J., 2011. Investigation of the Heating Rate Dependency  
568 Associated with the Loss of Crystalline Structure in Sucrose, Glucose, and Fructose  
569 Using a Thermal Analysis Approach. *J. Agric. Food Chem.* Vol. 59(2), 684–701.

570 Liu, Y., Ng, P.K.W., 2015. Isolation and characterization of wheat bran starch and endosperm  
571 starch of selected soft wheats grown in Michigan and comparison of their  
572 physicochemical properties. *Food Chem.* Vol. 176, 137–144.

573 Makhatadze, G.I., Privalov, P.L., 1995. Energetics of protein structure. *Adv. Protein Chem.*  
574 Vol. 47, 307–425.

575 Mann, J., 1971. Deuteration and titration. *Cellul. Cellul. Deriv.* Vol. 5(4).

576 Mochochoko, T., Oluwafemi, O.S., Jumbam, D.N., Songca, S.P., 2013. Green synthesis of  
577 silver nanoparticles using cellulose extracted from an aquatic weed; water hyacinth.  
578 *Carbohydr. Polym.* Vol. 98(1), 290–294.

579 Muztar, A.J., Slinger, S.J., Burton, J.H., 1978. The chemical composition of aquatic  
580 macrophytes. II. Amino acid composition of the protein and non-protein fractions.  
581 *Can. J. Plant Sci.* Vol. 58(3), 843–849.

582 Nishiyama, Y., Langan, P., Chanzy, H., 2002. Crystal structure and hydrogen-bonding system  
583 in cellulose II-beta from synchrotron X-ray and neutron fiber diffraction. *J Am Chem*  
584 *Soc* Vol. 124, 9074–9082.

585 Nishiyama, Y., Sugiyama, J., Chanzy, H., Langan, P., 2003. Crystal structure and hydrogen  
586 bonding system in cellulose II-alpha from synchrotron X-ray and neutron fiber  
587 diffraction. *Am Chem Soc* Vol. 125, 14300–14306.

588 Nivresse, A.-L., Thibault de Chanvalon, A., Baglan, N., Montavon, G., Granger, G., Péron, O.,  
589 2020. An overlooked pool of hydrogen stored in humic matter revealed by isotopic  
590 exchange: implication for radioactive <sup>3</sup>H contamination. *Environ. Chem. Lett.* Vol.  
591 18(2), 475–481.

592 Péron, O., Fourré, E., Pastor, L., Gégout, C., Reeves, B., Lethi, H.H., Rousseau, G., Baglan,  
593 N., Landesman, C., Siclet, F., Montavon, G., 2018. Towards speciation of organically  
594 bound tritium and deuterium: Quantification of non-exchangeable forms in  
595 carbohydrate molecules. *Chemosphere* Vol. 196(1), 120–128.

596 Péron, O., Gégout, C., Reeves, B., Rousseau, G., Montavon, G., Landesman, C., 2016.  
597 Anthropogenic tritium in the Loire River estuary, France. *J. Sea Res.* Vol. 118, 69–76.

598 Pointurier, F., Baglan, N., Alanic, G., Chiappini, R., 2003. Determination of organically  
599 bound tritium background level in biological samples from a wide area in the south-  
600 west of France. *J. Environ. Radioact.* Vol. 68(2), 171–189.

601 Richards, F.M., 1977. Areas, volumes, packing, and protein structure. *Annu. Rev. Biophys.*  
602 *Bioeng.* Vol. 6(1), 151–176.

603 Richardson, J.S., 1981. The anatomy and taxonomy of protein structure. *Acad. Press* Vol. 34,  
604 167–339.

605 Sakintuna, B., Budak, O., Dik, T., Yöndem-makascioglu, F., Kincal, N., 2003. Hydrolysis of  
606 freshly prepared wheat starch fractions and commercial wheat starch using  $\alpha$ -amylase.  
607 *Chem Eng Commun* Vol. 190, 883–897.

608 Sepall, O., Mason, S.G., 1961. Hydrogen exchange between cellulose and water: II.  
609 Interconversion of accessible and inaccessible regions. *Can. J. Chem.* Vol. 39(10),  
610 1944–1955.

611 Shulz, G.E., Schirmer, R.H., 2013. Principles of protein structure. Springer Sci. Bus. Media.

612 Sun, X.-F., Sun, R.-C., Su, Y., Sun, J.-X., 2004. Comparative Study of Crude and Purified  
613 Cellulose from Wheat Straw. *J. Agric. Food Chem.* Vol. 52(4), 839–847.

614 Sun, Y., Cheng, J., 2002. Hydrolysis of lignocellulosic materials for ethanol production: a  
615 review. *Bioresour Technol* Vol. 83, 1–11.

616 Tester, R.F., Karkalas, J., Qi, X., 2004. Starch composition, fine structure and architecture. *J*  
617 *Cereal Sci* Vol. 39, 151–165.

618 Van Soest, P.V., 1963. Use of detergents in the analysis of fibrous feeds. 2. A rapid method  
619 for the determination of fiber and lignin. *J. Assoc. Off. Agric. Chem.* Vol. 46, 829–  
620 835.

621 Verwimp, T., Vandeputte, G.E., Marrant, K., Delcour, J.A., 2004. Isolation and  
622 characterisation of rye starch. *J. Cereal Sci.* Vol. 39(1), 85–90.

- 623 Wuestenberg, T., 2014. Cellulose and Cellulose Derivatives. John Wiley Sons.
- 624 Xie, X. (Sherry), Cui, S.W., Li, W., Tsao, R., 2008. Isolation and characterization of wheat  
625 bran starch. Food Res. Int. Vol. 41(9), 882–887.
- 626 Zugenmaier, P., 2001. Conformation and packing of various crystalline cellulose fibers. Prog  
627 Polym Sci 1341–1417.
- 628
- 629

630 **Tables**

631

	(A-1)	(A-2)	(B-1)	(B-2)	(C-1)	(C-2)
<b>OBT (Bq.L<sup>-1</sup>)</b>	52.5 (±2.8)	32.7 (±2.5)	45.4 (±2.4)	25.6 (±1.9)	63.8 (±3.9)	14.2 (±1.9)
<b>OBT (Bq.kg<sup>-1</sup>)</b>	31.3 (±2.1)	18.4 (±2.0)	18.6 (±3.8)	11.8 (±1.6)	36.2 (±2.8)	8.9 (±1.2)

632

633 **Table 1:** Initial contents of organically bound tritium (OBT) in wheat grains (A-1), starch (A-  
 634 2), water-milfoil (B-1), cellulosic wall (B-2), apples (C-1) and simple carbohydrates (C-2)  
 635 matrices

636

637

638

	$\alpha_{model}$	(A-1)	(A-2)	(B-1)	(B-2)	(C-1)	(C-2)
<b>Starch</b>	30%	75.3 (±3.7)	85.1 (±2.1)	18.1 (±1.9)	7.6 (±0.9)	0.8 (±0.1)	-
<b>Maltose</b>	36.4%	-	14.9 (±2.1)	-	-	-	-
<b>Glucose</b>	41.7%	-	0.8 (±0.2)	-	-	17.3 (±0.9)	19.0 (±2.3)
<b>Fructose</b>	41.7%	-	-	-	-	51.0 (±1.5)	59 (±7.1)
<b>Sucrose</b>	36.4%	3.6 (±0.4)	-	0.8 (±0.8)	0.1 (±0.6)	19.9 (±0.6)	22.5 (±2.7)
<b>Cellulose</b>	30%	4.2 (±0.9)	-	16.5 (±1.5)	21.7 (±2.3)	3.7 (±1.6)	-
<b>Lignin</b>	17%	-	-	13.7 (±1.8)	26.2 (±3.0)	2.6 (±0.4)	-
<b>Hemicellulose</b>	27.1%	-	-	10.3 (±2.5)	19 (±7)	1.6 (±4.0)	-
<b>Protein<sup>(i)</sup></b>	37%	13.9 (±1.1)	-	-	-	-	-
<b>Protein<sup>(ii)</sup></b>	42%	-	-	37.3 (±2.7)	25.1 (±2.7)	-	-
<b>Fat</b>	< 0.1%	3.0 (±0.9)	-	3.2 (±1.3)	0.2 (±0.9)	0.9 (±0.9)	-

639

640 **Table 2:** The main essential components analyzed along with their associated theoretical  
 641 ( $\alpha_{model}$ ), and measured/analyzed distribution in % by weight in wheat grains (A-1), starch  
 642 (A-2), water-milfoil (B-1), cellulosic wall (B-2), apples (C-1) and simple carbohydrates (C-2)  
 643 matrices. <sup>(i)</sup> and <sup>(ii)</sup> are representative of wheat grains and water-milfoil protein types,  
 644 respectively.

645

646

	(A-1)	(A-2)	(B-1)	(B-2)	(C-1)	(C-2)
$\alpha_{model}$	30.0%	31.0%	31.5%	29.0%	38.7%	40.4%
$\alpha_{iso}$	31.0 ± 1.0%	31.1 ± 1.0%	26.4 ± 0.5%	16.1 ± 0.6%	28.0 ± 1.7%	39.6 ± 1.3%
$\alpha_{iso\ calculated}$	31.1 ± 0.8%	-	24 ± 15%	-	38 ± 10%	-
$\alpha_{iso\ calculated\ deviation}$	0.4 ± 0.1%	-	8.2 ± 5.1%	-	26 ± 7%	-

648

649 **Table 3:** Results of the molecular model-based theoretical exchangeable parameters  
650 ( $\alpha_{model}$ ), isotopic exchange based exchangeable parameter ( $\alpha_{iso}$ ) on wheat grains (A-1),  
651 starch (A-2), water-milfoil (B-1), cellulosic wall (B-2), apples (C-1) and simple carbohydrates  
652 (C-2) matrices, along with associated ( $\alpha_{iso\ calculated}$ ) parameters from extracted matrix  
653 results and the ( $\alpha_{iso\ calculated}$ ) deviation compared to actual ( $\alpha_{iso}$ ) parameters

654

655

656

657

	NE-OBT <sup>(a)</sup> (Bq.L <sup>-1</sup> )	NE-OBT <sup>(b)</sup> (Bq.L <sup>-1</sup> )	NE-OBT <sup>(b)</sup> (Bq.kg <sup>-1</sup> )	NE-OBT <sup>(b)</sup> distribution (%)	Distribution (% by weight)
<b>(A-1)</b>	33.1 (±3.6) <sup>(i)</sup>	33.1 (±2.6) <sup>(i)</sup>	19.7 (±1.6)	-	
<b>(A-2)</b>	32.2 (±1.5)	32.7 (±2.5)	18.6 (±1.4)	71.0 (±8.7)	75.3 (±3.7)
<b>(B-1)</b>	33.2 (±1.2)	33.7 (±3.1)	14.4 (±1.4)	-	
<b>(B-2)</b>	25.3 (±1.0)	24.6 (±2.3)	11.4 (±1.1)	44 (±22)	56 (±27)
<b>(C-1)</b>	24.9 (±3.3)	26.4 (±2.4)	15.8 (±1.5)	-	
<b>(C-2)</b>	16.0 (±2.6)	13.3 (±2.8)	8.4 (±1.8)	47 (±11)	88.2 (±5.9)

658

659 **Table 4:** Results obtained from (a) calculated and (b) NE-OBT concentration activities on the  
660 reference date of July 1, 2020 in wheat grains (A-1), starch (A-2), water-milfoil (B-1),  
661 cellulosic wall (B-2), apples (C-1) and simple carbohydrates (C-2) matrices, plus the  
662 calculated resulting distribution of NE-OBT vs. the distribution in % by weight of the  
663 constituents. <sup>(i)</sup>Results adapted from Péron *et al.* (2018).

664



665 **Figure**

666

667

668

669

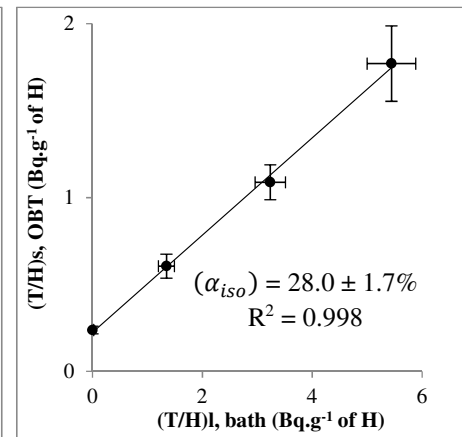
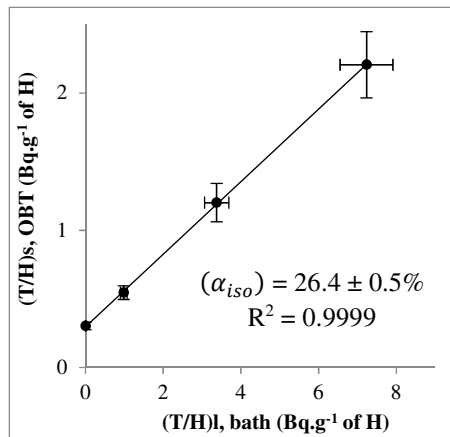
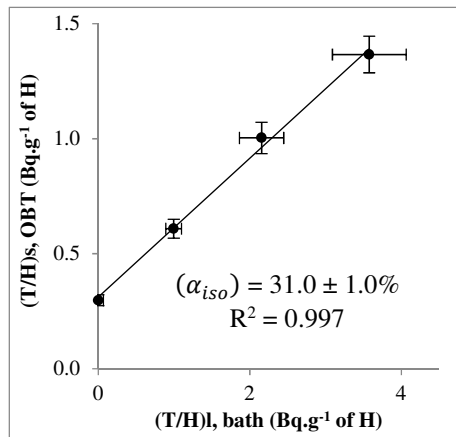
670

671

672

673

674



675

676

677

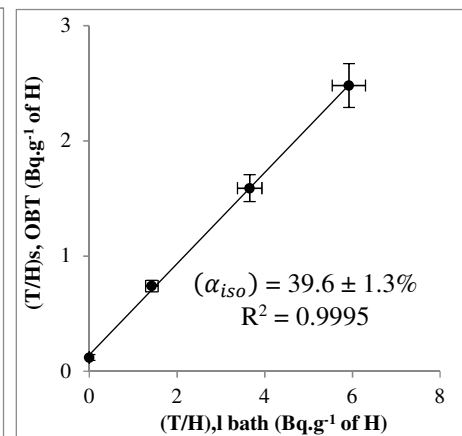
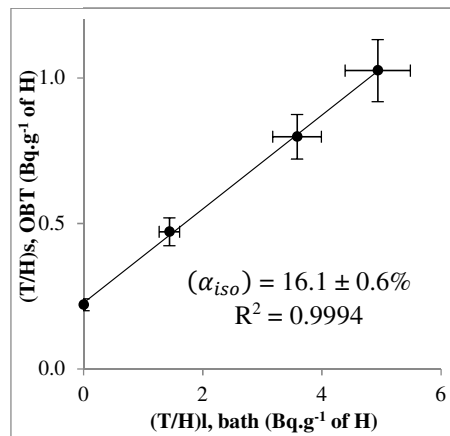
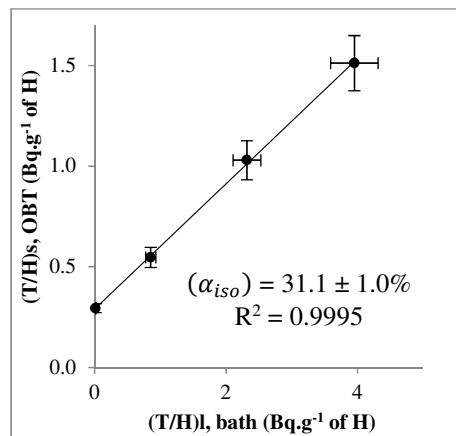
678

679

680

681

682



683

684

685

686

687

688

**Fig. 1:** (T/H) OBT at the steady state after freeze-drying vs. measured set (T/H) of saline solutions with the associated exchangeable hydrogen pool  $\alpha_{iso}$  parameter for: (a)\* wheat grains (A-1) (results from Péron *et al.* (2018)), (b) starch (A-2), (c) water-milfoil (B-1), (d) cellulosic wall (B-2), (e) apples (C-1), and (f) simple carbohydrates (C-2)